ELSEVIER

PII: S0032-3861(96)00987-1

Polymer Vol. 38 No. 16, pp. 4003–4009, 1997

0032-3861/97/$17.00+0.00

polymer papers

Morphology of poly(L-lactide) solution-grown crystals

Tadakazu Miyata* and Toru Masuko†
Faculty of Engineering, Yamagata University, 4-3-16 Jonan, Yonezawa, Yamagata 992, Japan
(Received 17 September 1996; accepted 14 October 1996)

Solution-grown crystals (SGC) of poly(L-lactide) (PLLA) were prepared from 0.01% (w/w) or 0.08% (w/w) acetonitrile solution by an isothermal crystallization method. Their morphology and structural features were examined by transmission electron microscope with the diffraction mode, wide-angle X-ray diffractometry and atomic force microscope. The molecular chains are packed in the manner perpendicular to the basal plane of the well-defined, lozenged, thin SGC with developed spiral dislocation growths; highly-ordered electron diffraction patterns produced by the crystal provided the orthorhombic unit cell parameters: $a = 1.078$ nm, $b = 0.604$ nm, c (fibre axis) $= 2.87$ nm. This unit cell of the PLLA SGC contains 20 monomeric units in terms of density measurements. On the basis of the crystal characteristics of SGC, we propose that the two molecular chains locate at the centre and also at each corner of the unit cell. The annealing effects of SGC were studied in parallel to indicate the existence of surface roughening and lamella thickening, depending on the annealing conditions. © 1997 Elsevier Science Ltd.

(Keywords: poly(L-lactide); structure; morphology)

INTRODUCTION

In the past several decades, widespread attention has been paid to the study of fibre- and film-forming polymeric materials. These investigations have mainly been carried out using polyolefin and other synthetic polymers. Since these polymer products may cause considerable environmental problems by reason of their chemical stability, studies of forming fibre and film from biodegradable crystalline polymers have become of increasing importance.

It is well known that poly(L-lactide) (PLLA) is a biodegradable and biocompatible crystalline polymer, with resultant environmental advantages among synthetic polymers. Other biodegradable synthetic polymers, such as poly(ϵ-caprolactone), polybutylene-succinate and polyglycolide, belong to crystalline aliphatic polyesters and are known for their usefulness as regards biodegradation.

Many investigations have been published on the degradation of PLLA both *in vitro* and *in vivo*[1–11]. In parallel with these investigations, several studies were carried out on the solid structure of PLLA[12–14] and the stereocomplex[15–17] of enantiomeric poly(lactide) by X-ray diffraction (X.r.d.) or conformational analysis of the molecular chains. The PLLA fibre has two crystal modifications, the α- and the β-form, depending on the spinning or drawing conditions[7,13]. De Santis and Kovacs[12] reported that the unit cell of the α-form PLLA structure is pseudo-orthorhombic with dimensions of $a = 1.07$ nm, $b = 0.645$ nm, $c = 2.78$ nm; the polymer chain may have a 10/3 helical conformation. However, this model was derived solely by the molecular transform technique, apart from rigorous calculation of the structure factor of each reflection. Hoogsteen *et al.*[13] discussed the helical chain models of PLLA involved in the pseudo-orthorhombic unit cell (the α-form; $a = 1.06$ nm, $b = 0.61$ nm, $c = 2.88$ nm), and argued that the result by DeSantis was not very likely.

In the latest X-ray work, Kobayashi *et al.*[14] showed that this type of helical chain locates on the α-form crystal, as evaluated by a fibre X-ray diffraction method, and examined the relationship between helical structure and physical properties for PLLA. Also, Brizzolara *et al.*[15] examined the packing mode of enantiomatic poly(lactide) chains, using the energetic computer simulation method. However, DeSantis and Kovacs[12] only compared an optical Fourier transform of their model with the pattern of an X-ray fibre photograph. Hoogsteen *et al.*[13] did not dispute the X-ray diffraction intensities. Neither the exact crystal structure nor the packing mode of the PLLA molecular chain, therefore, has been established in terms of atomic coordinates of the constituent elements. Thus it seems that the crystal structure of the PLLA-based 10/3 helix has not yet been established.

Independently, Fischer *et al.*[18] investigated solution-grown crystals (SGC) of lactide copolymer. Also, Kalb and Pennings[6] estimated the crystallization of PLLA from bulk state and solution. Neither group is yet clear on the morphology and crystal data of PLLA, nor have the crystal structure and molecular chain packing been investigated in their works.

In this report, we investigate the morphological

* Permanent address: Oji Paper Co. Ltd, R&D Division, Advanced Technology Research Laboratory, 1-10-6 Shinonome, Koto-ku, Tokyo 135, Japan
† To whom correspondence should be addressed

Table 1 Characteristics of PLLA usd in this work

i.r. absorption (cm^{-1})	C=O	ester	1760
	-O	ester	1190
^{1}H n.m.r. (ppm)	a	5.16	CH_3 O (-O-CH-C-)$_n$
	b	1.58	
g.p.c.		M_w =	1.6×10^5

features of solution-grown PLLA crystals, and examine the α-form crystal data. Our final purpose is to elucidate the relationship between the fine structure of PLLA and its physical properties in the bulk state.

EXPERIMENTAL

Polymer synthesis

Well-purified L,L-lactide (Tokyo Kasei Kogyo Co. Ltd, Japan) was kept in evacuated sealed tubes containing 0.03% (w/w) stannous octanoate (Sigma Chem. Corp., USA) and 0.01% (w/w) lauryl alcohol (Tokyo Kasei Kogyo Co. Ltd, Japan) as a catalyst activator and chain control agent[4]. The polymerization was carried out in a silicone oil bath at 220°C for 4 h. The solid polymer residue in the tube was dissolved in chloroform and then reprecipitated repeatedly from a large quantity of methanol at room temperature. The purified polymer thus obtained was white and fibrous in appearance. Results of its ^{1}H n.m.r. analysis, i.r. measurement and molecular weight obtained by gel permeation chromatography are listed in *Table 1*.

Preparation of solution-grown crystals

Solution-grown crystals (SGC) were precipitated from a 0.08% (w/w) or 0.01% (w/w) solution of polymer in acetonitrile, by isothermal crystallization at 25°C.

Annealed SGC were prepared by heat treatment at various temperatures in a nitrogen atmosphere in order to prevent them from degradation. A series of annealing experiments conducted on the PLLA crystals provided some interesting morphologies.

Film specimens

Quenched PLLA films were prepared by quenching them into ice water from a temperature above their respective T_ms. Crystallized PLLA films for X.r.d. measurements were made by heat treatment of the quenched film in an air oven at 100°C. Oriented samples were prepared by stretching quenched films to four times their length at 60°C, followed by annealing at 100°C.

Density measurements

Densities of the polymer films were determined using a flotation method in an aqueous $CaBr_2$ solution at 25°C.

Electron microscopy

Solution-grown crystals were placed on a carbon-coated sheet mesh and examined at 200 kV with a Philips CM-300 electron microscope. The surface of solution-grown specimens was shadowed with Au/Pd alloy, followed by replication with a carbon film.

X.r.d. measurements

Graphite-monochromatic CuKα radiation (λ = 0.15418 nm) was employed for X.r.d. experiments, using a MAC Science M18XHF-SRA generator operated at 50 kV and 350 mA. The X.r.d. photographs and integral intensities for both oriented and unoriented films were taken at room temperature using an imaging plate system (DIP-220). Spacings of the reflection planes were correlated with those of cholesterol standard powder.

Figure 1 PLLA crystals precipitated by isothermal crystallization of the 0.08% (w/w) solution in acetonitrile at 25°C

Atomic force microscopy

An atomic force microscopy (AFM) technique was selected as a primary method of measuring the thickness of solution-grown crystals with great precision. Unlike classic microscopic techniques, the AFM technique allows the acquisition of 3D topographic data with high vertical resolution in selected areas with lateral sizes on the nanometric scale.

A Seiko SPA-300 AFM with a SEIKO SPI-3800 probe station was employed at 23°C in this work. A rectangle-shaped silicon tip was applied in cyclic contact mode experiments with a spring contact force of 2.2 N m^{-1} and scan rates of 1–2 Hz.

RESULTS AND DISCUSSION

Morphology and structural properties of PLLA

A typical electron micrograph of PLLA SGC obtained from the acetonitrile solution is shown in *Figure 1*, where lozenge-shaped, stacked platelets are clearly observed. These crystals were obtained by isothermal crystallization from a 0.08% (w/w) acetonitrile solution. The size of the platelet was ca. 6 μm in the short direction, ca. 13 μm in the long direction, and the thickness of each crystal was 10–11 nm, measured from edge profiles using an AFM. However, since these crystals were stacked with heavy overgrowths, examination of their surface morphology is limited.

The size of PLLA SGC as a function of isothermal crystallization time at 25°C is shown in *Figure 2*, being directly proportional to crystallization time. Also, it is clear that the lamella platelets stack heavily with increasing crystallization time. It seems that an induction period of ca. 20 h exists for crystallization.

As is shown in *Figure 3*, adequately isolated crystals could be grown from a lower concentration solution (0.01% (w/w)) in acetonitrile. Well-defined SGC were also formed through spiral dislocation growth. The size of these crystals was ca. 3–7 μm, and they were 10–11 nm thick.

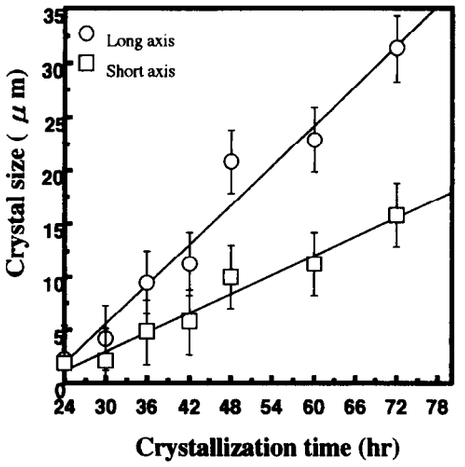

Figure 2 Changes in the size of PLLA solution-grown crystals as a function of isothermal crystallization time at 25°C

Figure 3 Well-defined PLLA crystals precipitated by isothermal crystallization of the 0.01% (w/w) solution in acetonitrile

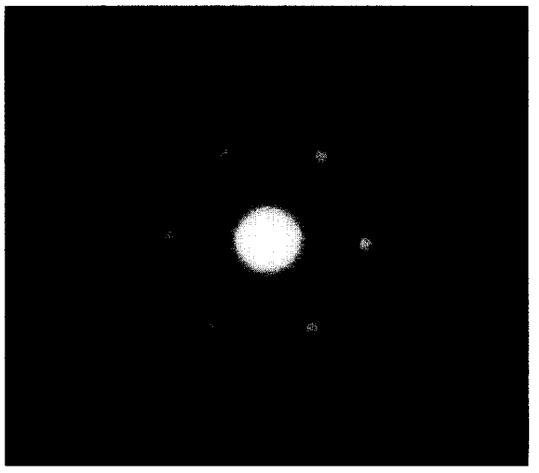

Figure 4 Selected-area electron diffraction pattern for the PLLA crystal

The SGC of various morphologies, including the sample in *Figure 3*, yield essentially the same electron diffraction (e.d.) pattern, as shown in *Figure 4*, the spot positions of which are illustrated schematically in *Figure 5*. The characteristic feature of this e.d. pattern is the fact

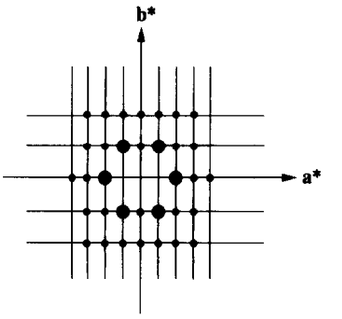

Figure 5 Schematic illustration of the electron diffraction pattern in *Figure 4* (a^* and b^* indicate the reciprocal lattice of this polymer)

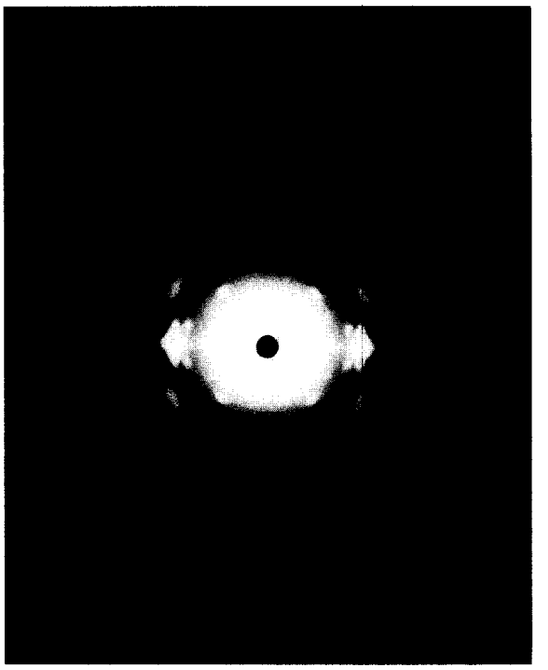

Figure 6 X-ray fibre photograph of the oriented PLLA film

that the (110) and (200) reflection is very strong and all others are weak, with a highly ordered pattern. All of the reflections can be indexed as (*hk*0) reflections based on the orthorhombic unit cell with dimensions $a = 1.078$ nm and $b = 0.604$ nm.

X-ray diffraction patterns of the oriented PLLA film specimens, *Figure 6*, were obtained at room temperature. In these fibre patterns ten layer lines are found, which give the repeating distance in the molecular chain axis as $c = 2.87$ nm. By use of the data above, the unit cell density is calculated to be $\rho_c = 1.285\,g\,cm^{-3}$ for PLLA crystals that possess 20 monomeric units in the orthorhombic cell. This value is consistent with the experimentally determined value $\rho_0 = 1.275\,g\,cm^{-3}$ for highly crystalline PLLA specimens. On the basis of this information, 20 monomeric units can be placed in the unit cell, and 10 monomeric units are presumably involved in the direction of the *c*-axis (fibre period). Two molecular chains of PLLA therefore pass through the unit cell.

The WAXD powder diagrams for the unoriented, annealed films indicate discrete diffraction lines that correspond to the *d* values shown in *Table 2*. These lines

Table 2 Observed X-ray *d*-spacings of PLLA

Observed *d*-spacings (nm)	Calculated[a] *d*-spacings (nm)	*hkl*
1.078	1.078	100
0.725	0.715	004
	0.714	103
0.607	0.604	010
0.538	0.539	200
	0.527	110
0.470	0.469	203
0.431	0.430	204
0.400	0.392	205
0.388	0.388	115
0.374	0.374	016
0.359	0.358	206
0.326	0.326	207
0.309	0.308	018
0.304	0.304	305
0.287	0.287	306
0.277	0.276	1010
0.275	0.274	209
0.270	0.270	307
		400
0.268	0.268	401
0.261	0.262	221
0.257	0.255	026

[a] $a = 1.078$ nm, $b = 0.604$ nm, $c = 2.87$ nm, *orthorhombic*

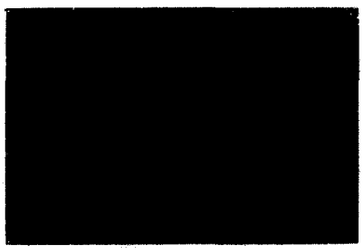

(a)

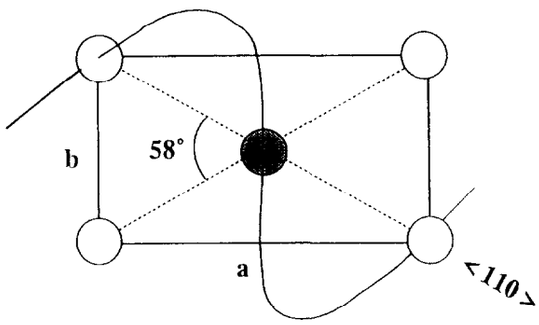

(b)

Figure 7 (a) Electron micrograph of PLLA solution-grown crystal. In the insert, a^* and b^* arrows indicate the reciprocal lattice of this polymer. (b) Schematic representation of the PLLA chain arrangement in the unit cell

Table 3 Crystal data of PLLA

Crystal system	orthorhombic
Cell dimensions:	
a (nm)	1.078
b (nm)	0.604
c (nm)	2.873
Density (g cm^{-3}):	
calc.	1.285
obs.	1.275
Number of monomeric units per unit cell	20

Table 4 Lattice constants of PLLA in previous reports

Authors	*a* (nm)	*b* (nm)	*c* (nm)	Crystal system	Ref.
De Santis and Kovacs	1.07	0.645	2.78	pseudo-orthorhombic	12
Kalb and Pennings	0.597	0.597		pseudo-hexagonal	6
	1.034	0.597		pseudo-orthorhombic	
Hoogsteen *et al.*	1.06	0.61	2.88	pseudo-orthorhombic	13
Kobayashi *et al.*	1.05	0.61	2.88	orthorhombic	14

(a)

(b)

Figure 8 Electron micrographs of (a) star-shaped PLLA crystals and (b) star-shaped PLLA crystal agglomerations

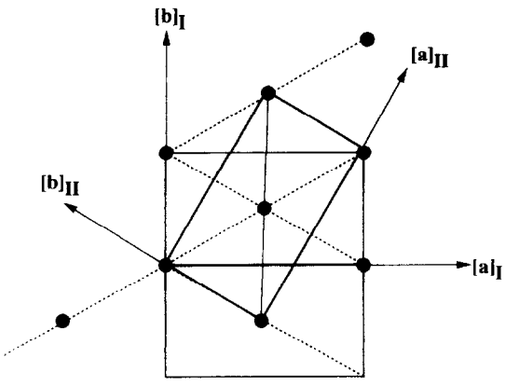

Figure 9 A proposed twinning of two PLLA solution-grown crystals. I and II indicate different crystals

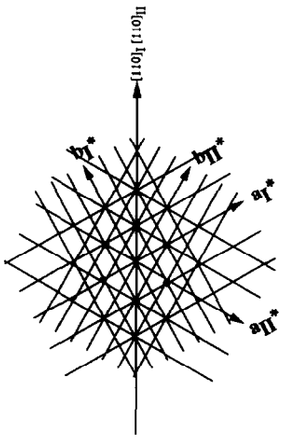

Figure 10 Schematic illustration of the electron diffraction pattern of the twin PLLA crystal (a^* and b^* indicate the reciprocal lattice of this polymer)

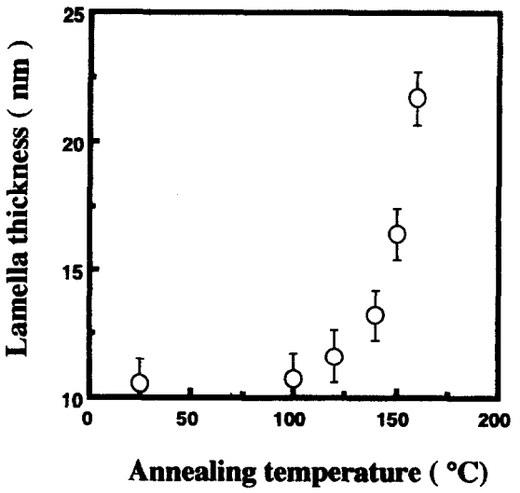

Figure 12 Lamellae thickness of PLLA annealing specimens (*Figure 11*) measured from edge profiles using an AFM

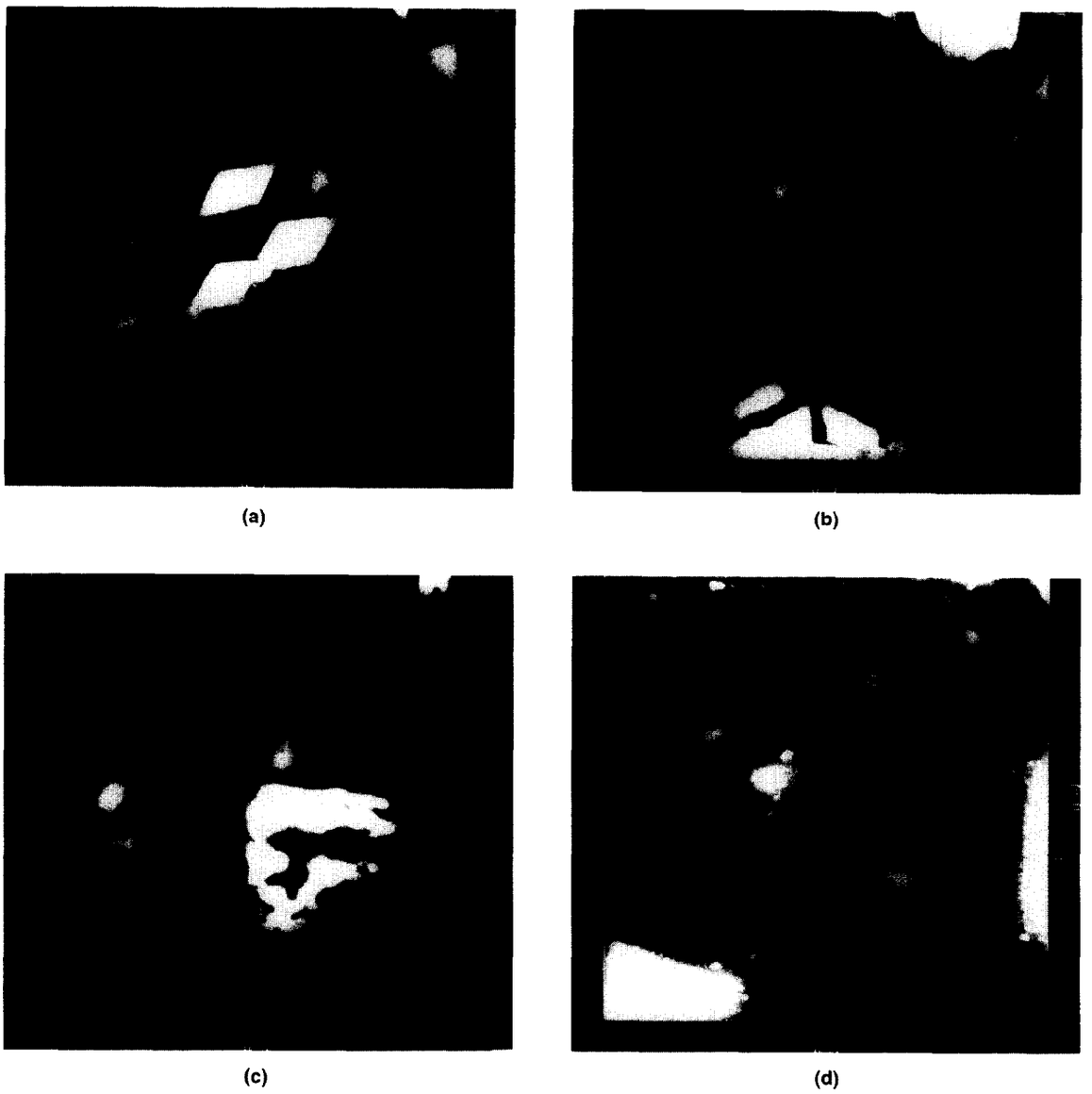

Figure 11 AFM images of PLLA crystals after annealing (a) at 120°C for 30 min, (b) at 140°C for 30 min, (c) at 160°C for 30 min, (d) at 180°C for 30 min

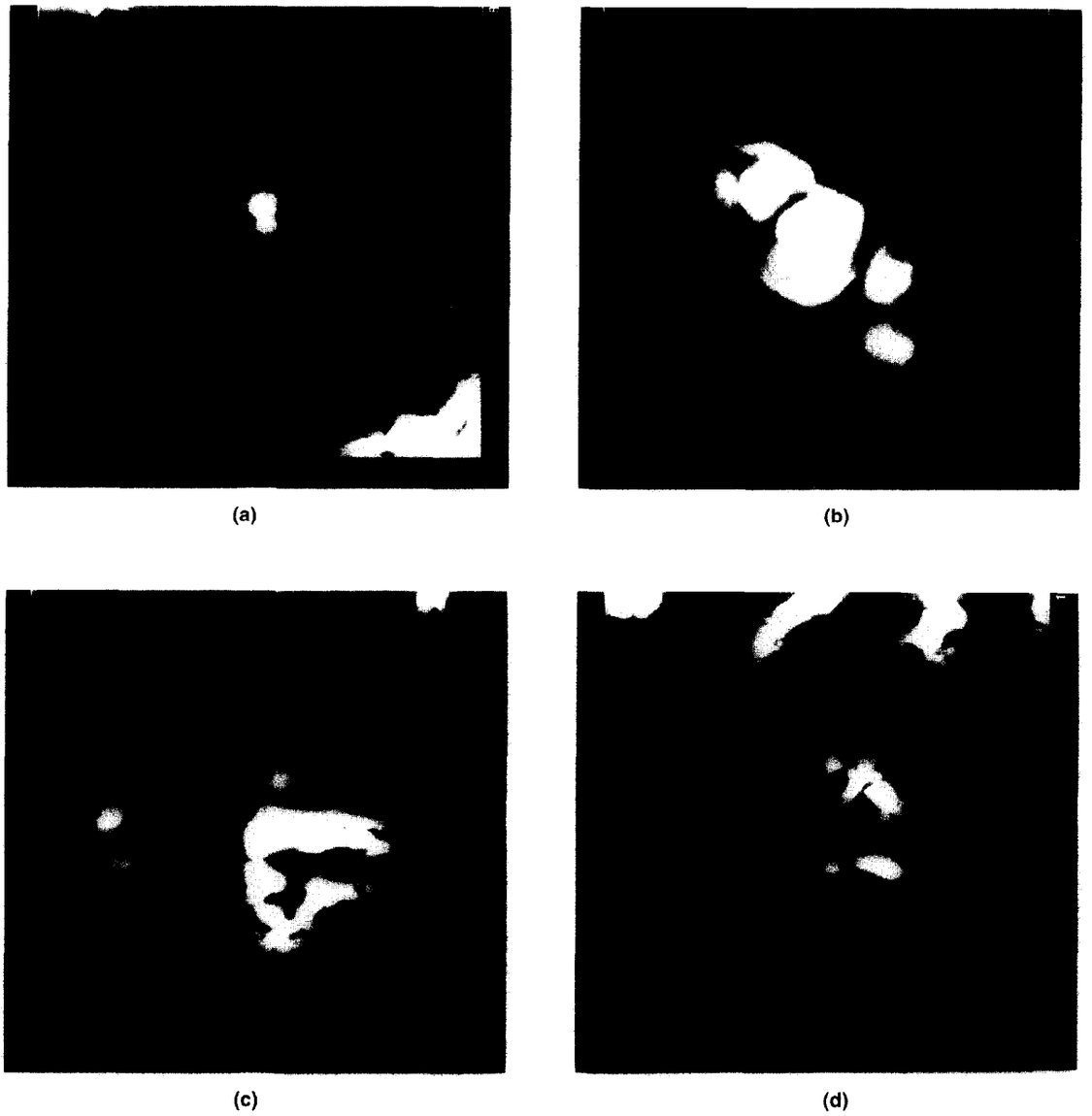

Figure 13 AFM images of crystals after annealing at 160°C for (a) 5 min, (b) 10 min, (c) 30 min and (d) 60 min

could be easily indexed using the lattice constants above, determined by electron diffraction. The indexed results also are summarized in *Table 2*, where the calculated d values from the lattice constants are compared with the observed X-ray values. This indicates good correspondence between two different methods.

Taking into account the systematic absence of the e.d. (*Figure 4*) and X.r.d. (*Figure 6*) reflections, the extinction rule cannot be applied. Thus, the orthorhombic space groups Pmm2–C_1^{2v}, P222–D_1^2 and Pmmm-D_1^{2h} could be selected. Fukada *et al.* discussed the chiral nature, optical activity and piezoelectric properties of this polymer[19–21]. It is known that crystal materials showing these physical properties are classified as a 'non-centrosymmetrical group'. However, the choice of space group is not satisfied with the symmetry of the helical chain. This problem will be discussed further in the near future.

Comparing the bright-field picture with the electron diffraction pattern on the SGC, we found that the a-axis locates in the diagonal direction of the lozenge-shaped crystal and the b-axis in the perpendicular direction to the a-axis. This feature is shown by the arrows in *Figure 7a*, and the situation is very similar to that observed in polyethylene single crystals. Therefore, folding of the molecular chain probably occurs along the $\langle 110 \rangle$ direction. The angle of 58° made by crossing of the (110) and ($1\bar{1}0$) planes is consistent with the acute angle formed by two counter lines as observed in *Figure 7a*. The molecular chains then pass through the centre and each corner of the unit cell (a–b plane), and the alternative configuration of the neighbouring chain could appear along the diagonal line (*Figure 7b*). This presumed chain arrangement is essentially not contradictory to that in the report by Kobayashi *et al.*[14].

The crystal data of this polymer are summarized in *Table 3*. The unit cell dimensions determined in the present study are essentially similar to those suggested earlier, as shown in *Table 4*.

Twinning in PLLA solution-grown crystals

In the PLLA SGC morphology there frequently appear star-shaped agglomerations of lamellae, or star-shaped

crystals, as shown in *Figures 8a* and *b*. The crystals grow along the diagonal ⟨110⟩ direction and produce, by merging, the broader platelet shown in these micrographs. Twinning is also noted in *Figure 9*. *Figure 10* illustrates the reciprocal net pattern of a typical electron diffraction pattern for the PLLA twinned crystals. This net pattern corresponds to the proposed twinning lattice geometry shown in *Figure 9*.

Annealing effects of PLLA solution-grown crystals

A series of annealing experiments on PLLA SGC was conducted and provides some interesting morphologies for those crystals. *Figure 11* shows a series of AFM images obtained after heat treatment at (a) 120°C for 30 min, (b) 140°C for 30 min, (c) 160°C for 30 min and (d) 180°C for 30 min, conducted in a nitrogen atmosphere in order to prevent the crystals from degradation. When examined in detail, these AFM images clearly show that erratic thickening and concomitant surface roughening of the crystals take place just below the isotopic melting point, 180°C. Further heating (above 180°C) resulted in melting of the SGC, followed by information of structures similar to those in *Figure 11d*. The lamellae thickness, measured from edge profiles using an AFM increases with increasing annealing temperature, as shown in *Figure 12*.

Also, *Figure 13* shows a series of AFM images obtained after heat treatment at 160°C for (a) 5 min, (b) 10 min, (c) 30 min and (d) 60 min in a nitrogen atmosphere. Morphologies of these crystals show that molecular refolding, lamella thickening and developing holes occur during the annealing process.

The annealing effects of PLLA SGC indicate that the existence of surface roughening and lamella thickening depends strongly on the annealing conditions. Interest is therefore invoked to examine the morphologies of PLLA solution-grown crystal mats. Detailed observation of morphologies and structural properties of the bulk PLLA will be discussed elsewhere[22].

CONCLUSIONS

The morphology and structural features of poly(L-lactide) (PLLA) have been studied by electron microscopy, X-ray diffraction and atomic force microscopy. The results obtained are as follows:

1. Well-defined, lozenged thin crystals of PLLA were precipitated by slow cooling of its dilute solution in acetonitrile. Spiral dislocation growths on the crystal were clearly observed, as well as twin PLLA crystals with a (110) twin plane.
2. The unit cell of this polymer shows the orthorhombic form with the following crystallographic parameters: $a = 1.078$ nm, $b = 0.604$ nm, c (fibre axis) $= 2.87$ nm. The two molecular chains are expected to locate at the centre and also at each corner of the unit cell. This unit cell of the PLLA crystal contains 20 monomeric units.
3. The annealing effects of PLLA solution-grown crystals indicate the existence of surface roughening and lamella thickening, depending on the annealing conditions.

ACKNOWLEDGEMENTS

The authors appreciate the contributions of Mr Kazuo Sasaki of Yamagata University, who has carried out some parts of the X-ray work and materials arrangements, and Mr Masuo Kudo of Yamagata University for his help in the AFM experiments.

REFERENCES

1. Kulkarni, R. K., Moore, E. G., Hegyeli, A. F. and Fredleonard, *J. Biomed. Mater. Res.*, 1971, **5,** 169.
2. Brady, J. M., Cutright, D. E., Miller, R. A., Bottistone, G. C. and Hunsuck, E. E., *J. Biomed. Mater. Res.*, 1973, **7,** 155.
3. Miller, R. A, Brady, J. M. and Cutright, D. E., *J. Biomed. Mater. Res.*, 1977, **11,** 711.
4. Gilding, D. K. and Reed, A. M., *Polymer*, 1979, **20,** 1459.
5. Reed, A. M. and Gilding, D. K., *Polymer*, 1981, **22,** 494.
6. Kalb, B. and Pennings, A. J., *Polymer*, 1980, **21,** 607.
7. Eling, B., Gogolewski, S. and Pennings, A. J., *Polymer*, 1982, **23,** 1587.
8. Zwiers, R. J. M., Gogolewski, S. and Pennings, A. J., *Polymer*, 1983, **24,** 167.
9. Eenink, M. J. D., Feijin, J., Olijslager, J., Albers, J. H. M., Riek, J. C. and Geidanus, P. J., *J. Controlled Release*, 1987, **6,** 225.
10. Kimura, Y., Matsuzaki, Y., Yamane, H. and Kitao, T., *Polymer*, 1989, **30,** 1342.
11. Reeve, M. S., McCarthy, S. P., Downey, M. J. and Gross, R. A., *Macromolecules*, 1994, **27,** 825.
12. De Santis, P. and Kovacs, A. J., *Biopolymers*, 1968, **6,** 299.
13. Hoogsteen, W., Postema, A. R., Pennings, A. J., tenBrinke, G. and Zugenmaier, P., *Macromolecules*, 1990, **23,** 634.
14. Kobayashi, J., Asahi, T., Ichiki, M., Okikawa, A., Suzuki, H., Watanabe, T., Fukada, E. and Shikinami, Y., *J. Appl. Phys.*, 1995, **77,** 2957.
15. Brizzolara, D., Cantow, H. J., Diederichs, K., Keller, E. and Domb, A. J., *Macromolecules*, 1996, **29,** 191.
16. Ikada, Y., Jamshidi, K., Tsuji, H. and Hyon, S. H., *Macromolecules*, 1987, **20,** 904.
17. Okihara, T., Tsuji, M., Kawaguchi, A., Katayama, K., Tsuji, H., Hyon, S. H. and Ikada, Y., *J. Macromol. Sci.—Phys.*, 1991, **B30,** 119.
18. Fischer, E. W., Sterzel, H. J. and Wegner, G., *Kollo.-Z. Z. Polym.*, 1973, **251,** 980.
19. Ichiki, M., Asahi, T., Watanabe, T., Kobayashi, J. and Fukada, E., *Repts. Progr. Polym. Phys. Jpn.*, 1992, **35,** 441.
20. Ichiki, M., Watanabe, T., Asahi, T., Kobayashi, J. and Fukada, E., *Repts. Progr. Polym. Phys. Jpn.*, 1992, **35,** 445.
21. Fukada, E., *Repts. Progr. Polym. Phys. Jpn.*, 1991, **34,** 269.
22. Miyata, T. and Masuko, T., *Polymer* (submitted for publication).